



HAL
open science

Small molecules organic photovoltaic devices based on the planar heterojunction porphyrin derivatives/fullerene

Jorge H. Velez, M. Jesus Aguirre, Linda Cattin, Mohammed Makha, Christian Bernède

► To cite this version:

Jorge H. Velez, M. Jesus Aguirre, Linda Cattin, Mohammed Makha, Christian Bernède. Small molecules organic photovoltaic devices based on the planar heterojunction porphyrin derivatives/fullerene. *Journal of Porphyrins and Phthalocyanines*, 2014, 18, pp.347-432. 10.1142/S1088424613501253 . hal-03350409

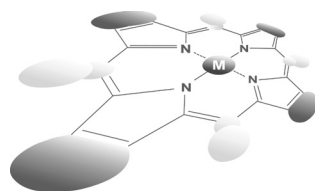
HAL Id: hal-03350409

<https://univ-angers.hal.science/hal-03350409>

Submitted on 21 Sep 2021

HAL is a multi-disciplinary open access archive for the deposit and dissemination of scientific research documents, whether they are published or not. The documents may come from teaching and research institutions in France or abroad, or from public or private research centers.

L'archive ouverte pluridisciplinaire **HAL**, est destinée au dépôt et à la diffusion de documents scientifiques de niveau recherche, publiés ou non, émanant des établissements d'enseignement et de recherche français ou étrangers, des laboratoires publics ou privés.



Small molecules organic photovoltaic devices based on the planar heterojunction porphyrin derivatives/fullerene

Jorge H. Velez^{*a,b}, M. Jesús Aguirre^a, Linda Cattin^c, Mohammed Makha^{dt} and Jean C. Bernede^d

^a Universidad de Santiago de Chile, Departamento de química y biología, laboratorio de polímeros conductores, Av. Libertador O'Higgins 3363, Estación Central, Santiago, Chile

^b Universidad Diego Portales, Facultad de Ingeniería, Av. Ejército 441, Santiago, Chile

^c Université de Nantes, Institut des Matériaux Jean Rouxel (IMN), CNRS UMR 6205, 2 rue de la Houssinière, BP 32229, 44322 Nantes cedex 3, France

^d Université d'Angers, MOLTECH-Anjou, CNRS UMR 6200, 2 Bd Lavoisier, 49045 Angers cedex, France

ABSTRACT: In this paper, we studied of photoelectric properties of multilayer organic photovoltaic cells (OPV cells). The active organic layers consisted of a planar heterojunction between a layer of (*meso*-tetrakis(5-bromo-2-thienyl)porphyrin), (TBrTP) as electron donor (ED) and a layer fullerene molecules. For the manufacture of photovoltaic devices we use a the technique of high vacuum by thermal sublimation that allows multilayer devices realization easily by successive depositions, and it does not require solvents, achieving purer films with reproducible characteristics. The TBrTP allows achieving OPVCs exhibiting promising efficiencies when the ABL is the MoO₃/CuI DABL. The CuI improves the current in the organic layer by one order of magnitude, which allows decreasing the series resistance of the OPVCs and therefore improving the OPVCs.

KEYWORDS: porphyrin derivative, organic solar cell, planar heterojunction.

INTRODUCTION

Following the success of organic light emitting diodes (OLEDs), a growing interest is dedicated to organic photovoltaic cells (OPVCs). To date all the OLEDs available on the market are realized by joule heating under vacuum. So active materials based on small molecules are the focus of increasing interest for the fabrication of organic solar cells. In fact compared to polymers, small molecules allow the development of reproducible synthesis purification and process [1].

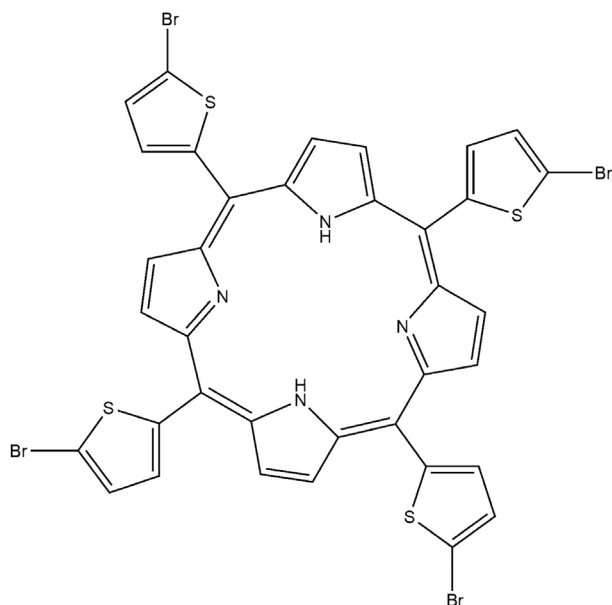
The realization of OPVCs by vacuum deposition presents the advantage of simple fabrication of multilayer devices and easy control of the layers thickness [2]. A classical planar heterojunction OPVCs cell involves

a bilayer of donor and acceptor material sandwiched between transparent and metal electrodes. The light absorbing layer is generally the electron donor (ED) like for example a metal phthalocyanine (MPc) associated with an electron acceptor (A), such as fullerene C60 [3]. If MPc have been broadly studied, porphyrin and its derivatives, which are also well-known dyes have not been so often studied. As a matter of fact, up to now the study dedicated to porphyrin derivatives were mainly dedicated to metal porphyrin derivatives [4, 5]. In the present work we show that a quite simple porphyrin derivative (*meso*-tetrakis(5-bromo-2-thienyl)porphyrin), (TBrTP) (Scheme 1), can be used with promising success as ED in OPV.

The earth of the OPVCs studied in the present work is based on the planar heterojunction Porphyrin derivatives/fullerene. However additional films are necessary to grow performing devices. Beyond electrodes, other layers turn out to be necessary to obtain successful OPVCs. Indeed, it is necessary to improve the contact electrodes/organic materials, which is often achieved through the introduction

*Correspondence to: Jorge Velez, email: jorge.velez@usach.cl

†Current address: Laboratoire Optoélectronique et Physico-chimie des Matériaux, unité de recherche associé au CNRST-URAC-14-Université Ibn Tofail, Faculté des Sciences BP 133 Kenitra 14000, Morocco



Scheme 1. Molecule of (*meso*-tetrakis(5-bromo-2-thienyl)-porphyrin), (TBrTP)

of a thin buffer layer at the interface. In the present work, the transparent conductive anode is the classical ITO, while the cathode is the often used aluminum. The buffer layer on the cathode side, usually called exciton blocking layer (EBL) [6], is an Alq₃ thin film, thick of 8 nm. Bathocuproine (BCP) is often used as exciton blocking buffer layer [6], however, in the present work, the aluminum tris(8-hydroxyquinoline) (Alq₃) has been chosen because it has been shown that it allows to grow solar cells with higher lifetime [7, 8]. About the interface ITO/ED it is well known that it is necessary to improve the band matching between the anode and the organic material, in order to achieve efficient hole collection. If high work function buffer layer such as PEDOT/PPS [9] and Au [10] are known to improve efficiently the band matching at the interface ITO/ED, we have shown that MoO₃ is very efficient whatever the highest occupied molecular orbital (HOMO) value of the ED [11]. Therefore it was used as anode buffer layer (ABL) in the present OPVCs. However, if MoO₃ [12] allows achieving a good band matching between ITO and the ED, it was shown that some others specific materials, such as PTCDA [13] or CuI [14] allow to modify the structure of the ED and therefore, to improve the solar OPVCs performances. In a recent work [15], we showed that, by using double anode buffer layer (DABL) it is possible, not only to improve the band matching at the interface, but to also to modify the structure of the ED in such a way that devices with higher current density and open circuit voltage are achieved. This DABL consist in a thin film of MoO₃ (3 nm) recovered by a thin CuI layer (1.5 nm). We assume the reason for this may be due to the dual function of MoO₃ and CuI since both of them were reported to be able to reduce the hole injection barrier compared with bare ITO, while CuI improve the ED films

morphology and conductivity while MoO₃ prevents the OPV cells from leakage path formation. Therefore the typical OPVCs of the present work are as follow:

Glass/ITO/ABL/TBrTP/C60/Alq₃/Al, with ABM = MoO₃ or MoO₃/CuI.

EXPERIMENTAL

Synthesis and characterization of the porphyrin derivatives

Chemical reactives. All the reactives and solvents used where pro analysis quality: pyrrole and 5-bromo-2-thiophenecarboxaldehyde for synthesis were obtained from Sigma-Aldrich; propionic acid p.a. from Merck; hexane p.a., chloroform p.a., ethanol p.a., methanol p.a., sodium hydroxide p.a., acetone p.a., acetic acid 100% p.a., boric acid, orthophosphoric acid 85%, silica gel 60 230–400 mesh ASTM, 0.04–0.063 mm porosity, for column, cobalt acetate(II), deuterated chloroform and sodium sulfite were from Merck; potassium chloride from Riedel-de-Haen; tetrabutylammonium perchlorate 99% from Across-Organics; silicone oil from Vetec; dichloromethane p.a. from J.T Baker; and ultra pure nitrogen 99.995 from AGA.

Instruments. Microanalysis was performed on a Fison, Model EA-1108 elemental analyzer. Proton nuclear magnetic resonance spectra (¹H NMR) were registered in a Bruker Advance 400 MHz spectrometer and processed by Mestrec software. UV-visible electronic spectra were registered in a Scinco S-3100 spectrophotometer, which has a diode bridge detector on 1 cm optical pass quartz cell. The equipment is controlled by the LabPro software through an interface. The spectrum window used was 350 to 750 nm. All the measurements were taken in dichloromethane at room temperature. The cyclic voltammograms were measured by a CH Instrument 604C potentiostat, connected to a computer, controlled by CHI software through interface. For pH measurements, it was used a pH-meter (HI 8424 HANNA Instruments).

Synthesis of (*meso*-tetrakis(5-bromo-2-thienyl)porphyrin), (TBrTP). The monomer was synthesized according to what is described in literature, Adler method. 5-bromo-2-thiophenecarboxaldehyde, 95% (2.6 mL, 2.1 × 10⁻² mol) and pyrrole 98% (1.5 mL, 2.1 × 10⁻² mol) in 150 mL of propionic acid were heated by reflux. In about 30 min, the formation of a black precipitate was observed. It was cooled at room temperature, and then methanol was added, cooling it by an ice bath at 0 °C during 15 min. Subsequently, it was filtered and the filtrand was washed with distilled water and methanol, dried and later purified by column chromatography (silica/CH₂Cl₂), obtaining a solid and crystalline purple precipitate (27% yield): TBrTP. Elemental analysis C₃₆H₁₈N₄S₄Br₄; calcd. C: 45.30, H: 1.90, N: 5.87; found C: 45.33, H: 1.84, N: 5.83. ¹H NMR (400 MHz, CDCl₃)

1 TTP: δ , ppm -2.71 (2H), 7.94–7.89 (4H, thiophene ring
2 hydrogens), 8.11–8.08 (4H, thiophene ring hydrogens),
3 9.27–8.88 (8H, porphyrin ring hydrogens).

4 5 **Organic photovoltaic cells realization and** 6 **characterization** 7

8 Before thin films deposition, the ITO coated glass
9 substrates were scrubbed with soap, rinsed with distilled
10 water, dried and next placed in the vacuum chamber
11 (10⁻⁴ Pa). The ABL, CuPc, C60, BCP and aluminum
12 layers were deposited sequentially onto the substrate by
13 sublimation or evaporation. Following an earlier study,
14 we chose to work with a CuI layer thick of 1.5 nm
15 and the deposition rate of CuI being 0.005 Å/s [16].
16 According to results previously obtained, the thickness
17 of the MoO₃ layer was 4 nm, that of C60 was 40 nm and
18 that of Alq₃ 8 nm [17]. In order to check the efficiency
19 of the DABL, reference OPVCs using MoO₃ alone as
20 ABL were also studied. The effective area of each cell
21 was 0.16 cm². The thin films thicknesses were estimated
22 *in situ* using a quartz monitor. The thickness of the ED
23 was varied from 18 nm to 8 nm.

24 Electrical characterizations were performed with an
25 automated I-V tester, in the dark and under sun global
26 AM 1.5 simulated solar illumination. Performances of
27 photovoltaic cells were measured using a calibrated solar
28 simulator (Oriel 300W) at 100 mW/cm² light intensity
29 adjusted with a PV reference cell (0.5 cm² CIGS solar
30 cell, calibrated at NREL, USA). Measurements were
31 performed in ambient atmosphere. All devices were
32 illuminated through TCO electrodes.

33 In order to determine the effect of the ABL on the organic
34 film conductivity, we have investigated the J-V charac-
35 teristics of hole-only devices with MoO₃ and MoO₃/CuI
36 ABL. These devices were grown using high work-function
37 electrode buffer layers. The hole only devices were
38 fabricated by replacing the C60 and the BCP EBL with
39 high the work function MoO₃, which is well-known to be a
40 hole injector (collector). Hole only devices have been made
41 using the same ITO covered glass substrate than those used
42 to grow OPV cells. After deposition of the ABL, an organic
43 film thick of 40 nm has been deposited. Then the organic
44 film has been covered with a MoO₃ film thick of 7 nm.
45 Finally aluminum has been used as top electrode.

46 47 **Thin films characterization** 48

49 In order to understand the effect of the different ABL
50 on the OPV cells performances, different characterization
51 techniques have been used for studying the structures
52 ITO/ABL/TTB.

53 The thin films structures are analyzed by X-ray
54 diffraction (XRD) by a Siemens D5000 diffractometer
55 using K α radiation from Cu ($\lambda K\alpha = 0.15406$ nm).

56 The film transmittance was measured at wavelengths
57 of 1.2 to 0.30 μ m. The optical measurements were

1 carried out at room temperature using a Carry spectrom-
2 eter. The morphology of the different structures
3 used as anode was observed through scanning electron
4 microscopy (SEM) with a JEOL 7600F at the “Centre de
5 Microcaractérisation de l’IMN, Université de Nantes”.
6 Images in secondary (SEM) and backscattering (BEI)
7 mode have been done.

8 Atomic Force Microscope (AFM) images on different
9 sites of the film were taken *ex-situ* at atmospheric
10 pressure and room temperature. All measurements have
11 been performed in tapping mode (Nanowizard III, JPK
12 Instruments). Classical cantilevers were used (Type PPP-
13 NCHR-50, Nanosensor). The average force constant and
14 resonance were approximately 14 N/m and 320 kHz,
15 respectively. The cantilever was excited at its resonance
16 frequency.

17 18 **RESULTS AND DISCUSSION** 19

20 21 **OPVCs study** 22

23 The carrier mobility in organic material being very
24 small, the thickness of the organic layers strongly affects
25 the performances of OPVCs. The optimization of the
26 thickness of the others organic layers having already
27 been realized, that of TBrTP has been used as parameter.
28 We can see in Table 1 that, actually, the power conversion
29 efficiency (PCE) of the OPVCs depends strongly on the
30 thickness of the TBrTP layer. It increases from 0.2% to
31 1.32% when the TBrTP film thickness decreases from
32 18 nm to 10 nm. For thinner TBrTP film (8 nm) there is
33 no more increase of the PCE.

34 The improvement of the performances corresponds
35 to an increase of all the OPVCs parameters (Table 1).
36 It must be noted that these OPVCs performances were
37 systematically achieved with the DABL. A comparison
38 of the results obtained with MoO₃ and MoO₃/CuI after
39 optimization of the TBrTP thickness is shown in Fig. 1,
40 while, in Table 1, it can be seen that the efficiency
41 obtained with MoO₃/CuI DABL is nearly the double of
42 that obtained with MoO₃ alone. One can see that the open
43 circuit voltage Voc and the short circuit current Jsc are
44 strongly improved, while the fill factor FF is slightly
45 smaller.

46 Having optimized the thickness of the TBrTP
47 layer, we studied the influence of the CuI layer on the
48 performances of the OPVCs. As a matter of fact, the
49 efficiency of the OPVCs decreases systematically with
50 the increase of the CuI layer thickness beyond 1.5 nm.
51 For instance for a thickness of 4 nm of CuI in the DABL,
52 the PCE of the cells was only 0.58%, with Voc = 0.34 V,
53 Jsc = 3.5 mA/cm² and FF = 40%. This shows that the
54 main contributions to the OPVCs performances are due
55 to Voc and FF.

56 In order to compare the effects of CuI and MoO₃/
57 CuI on the performances of the OPVCs, the ITO/

Table 1. Typical parameters of organic solar cells with different TBrTP thicknesses

ABL	TBrTP, nm	Voc, V	Jsc, mA/cm ²	FF, %	η , %	Rs	Rsh
MoO ₃ /CuI	18	0.40	1.18	44.5	0.20	29	630
MoO ₃ /CuI	15	0.44	2.9	48	0.61	11.5	600
MoO ₃ /CuI	12	0.54	3	52	0.84	10	880
MoO ₃ /CuI	10	0.56	4.4	54	1.32	7.4	600
MoO ₃ /CuI	8	0.54	4.2	53	1.20	6	600
MoO ₃	10 nm	0.43	2.77	59	0.7	6	1100

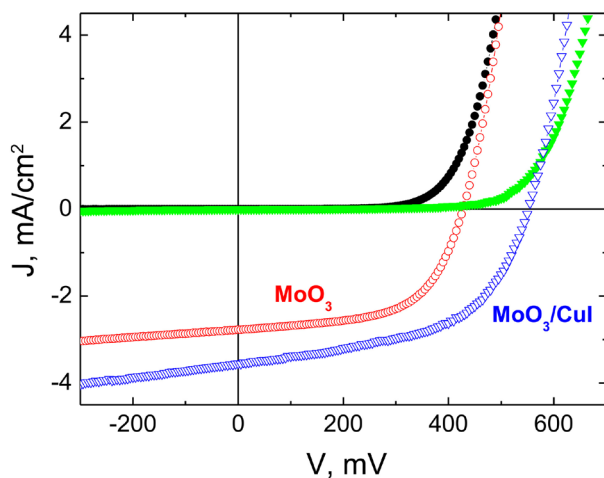


Fig. 1. Typical J-V characteristics of ITO/ABL/TBrTP (10 nm)/C₆₀/Alq₃/AIOPVCs, with ABL = MoO₃ (●), and MoO₃/CuI (▼), in the dark (full symbol) and under illumination of AM1.5 solar simulation (100 mW/cm²) (open symbol)

MoO₃/CuI/TBrTP and ITO/CuI/TBrTP devices have been characterized by UV-Vis spectroscopy, electrical measurement, X-ray diffraction, scanning electron microscopy and AFM.

Characterization of the ITO/ABL/TBrTP structures

Optical and electrical properties. The absorption of the TBrTP films (20 nm) deposited onto ITO and the different ABL is reported in Fig. 2.

The absorption spectrum for the ligand shows a Soret band (β) on the 380 nm to 490 nm region, and over the 480 nm 4 bands (Q) can be observed. This intense absorption bands are characteristic for porphyrins and are due to π - π^* ligand transitions.

About the effect of the ABL, as shown in Fig. 2, the absorption spectra of the TBrTP films (30 nm) deposited on ITO/CuI/MoO₃ and ITO/CuI exhibit some difference induced by the ABL. Figure 2 shows that if there is a small blue shift of the absorption range of TBrTP when deposited onto the MoO₃/CuI DABL, there is also a significant improvement of its absorbance. Moreover the shape of the absorbance spectrum is modified.

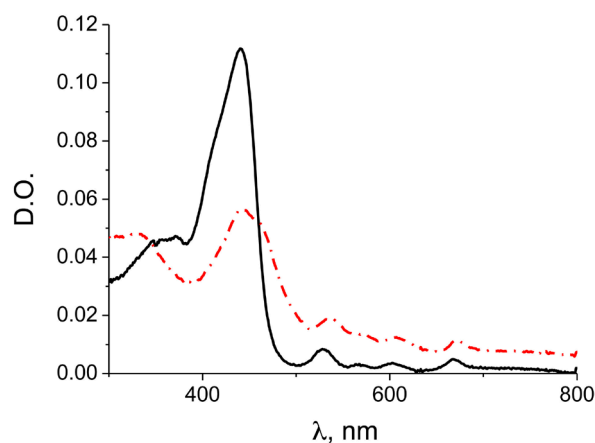


Fig. 2. Optical density spectra of TBrTP thin films (20 nm) deposited onto ITO/CuI (—) and ITO/MoO₃ (---) anodes density spectrum

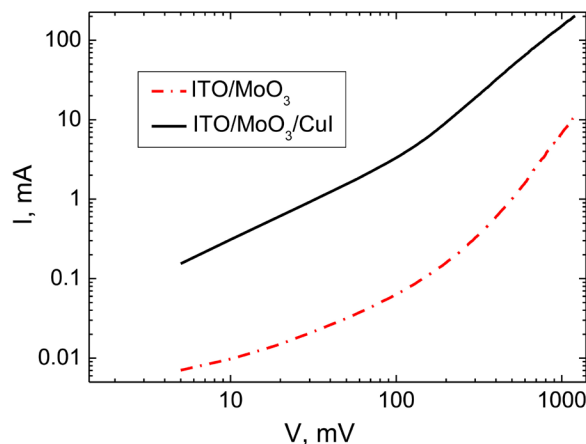


Fig. 3. Log-log plot of the current density-voltage curves of the hole only devices: ITO/ABL/TBrTP/MoO₃/Al, ABL = MoO₃ (---) or MoO₃/CuI (—)

Also, the conductivity of the hole only devices depends on the ABL. It is one order of magnitude higher when the TBrTP film is deposited onto MoO₃/CuI DABL (Fig. 3).

Structural properties. If the X-ray diffraction diagrams of these various films do not indicate any crystallinity of the TBrTP (not shown), the MEB and AFM studies show

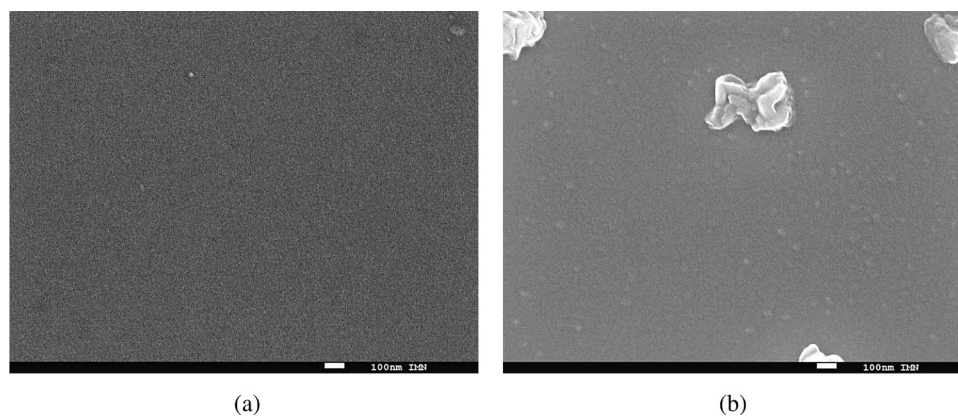


Fig. 4. Scanning electron microphotography of a TBrTP layer deposited onto CuI (a) and MoO₃/CuI (b)

that the morphology of the TBrTP films depends strongly on the ABL.

As shown in Fig. 4 the surface morphology of the TBrTP layers depends strongly on the ABL. The layers are homogeneous when they are deposited onto the MoO₃/CuI DABL, while large features of 0.12 to 0.16 μm² are randomly distributed at the surface of the layers deposited onto MoO₃.

In order to check if these features correspond to the polymer or some other compound, we have visualized in

Fig. 5 the same surface in the secondary electron mode and in the backscattering mode. In that mode, the lighter atoms appear darker on the photos. The features appear darker than the film itself, which means that the features visible in the secondary electron mode correspond in heap of TBrTP. The presence of these heaps is confirmed by the AFM study.

In Fig. 6, the AFM images in three dimensions of the TBrTP film deposited onto MoO₃ show clearly the presence of the features already visualized by SEM.

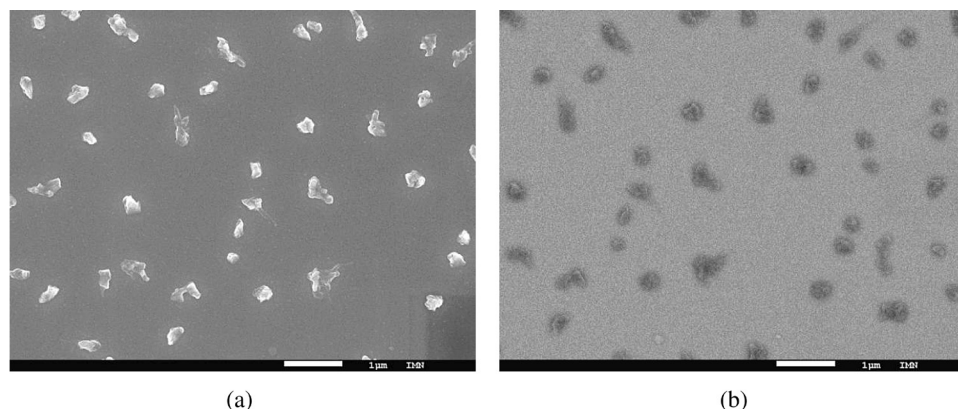


Fig. 5. Image in the secondary (a) and backscattering mode (b) of the surface of ITO/MoO₃/TBrTP structures

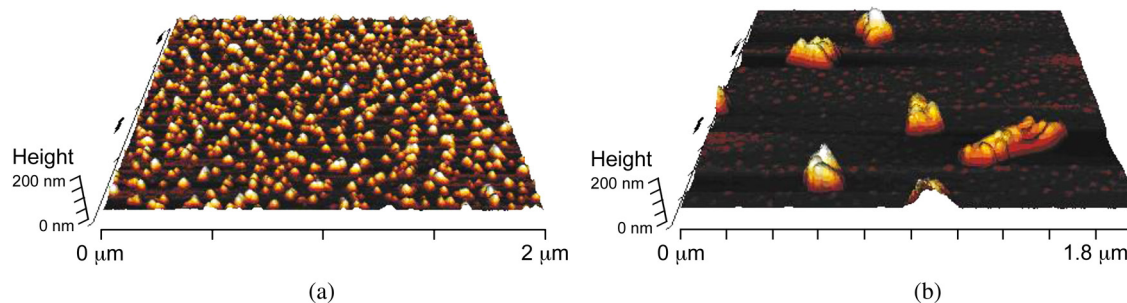


Fig. 6. AFM images in three dimensions of a TBrTP layer deposited onto CuI (a) and MoO₃/CuI (b)

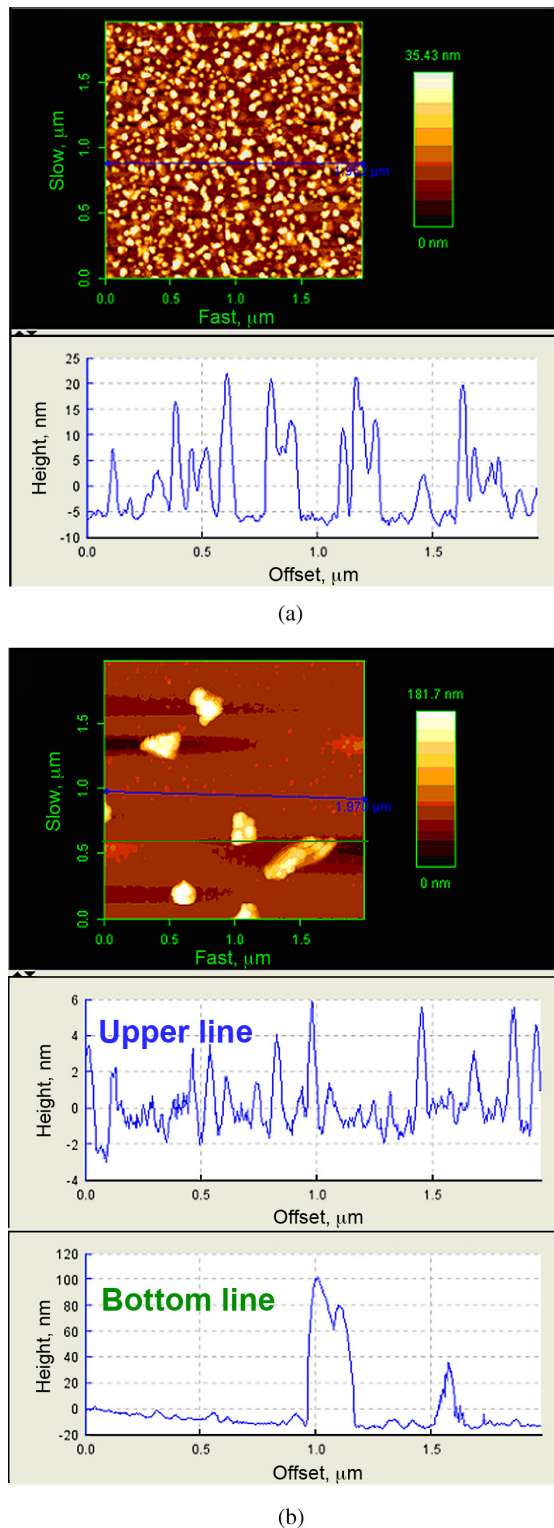


Fig. 7. Two dimensions AFM images and profiles of TBrTP films deposited onto ITO/MoO₃/CuI (a) and ITO/MoO₃ (b) structures

In the case of the films deposited onto MoO₃/CuI a high density of small heaps are distributed all over the surface.

The profiles of Fig. 7 allow measurement of the height of these different heaps. In the case of the TBrTP films

deposited onto MoO₃, when the profile is crossed so that it does not cut any feature (Fig. 7, upper line), the maximum height of peaks is of 6 nm, but when it crosses a feature (bottom line), the maximum height is 100 nm. In the case of the TBrTP films deposited onto MoO₃/CuI (Fig. 7a), the maximum height of peaks is 20 nm and the rms 7.5 nm, while it is 37 nm in the case of MoO₃ ABL (Fig. 7b). This high rms value is due to the broad features present at the surface of the films.

DISCUSSION

The classical equivalent electrical scheme of OPV cells was used to calculate, the shunt resistance, R_{sh} , defined by the slope of the J-V curve at $J = J_{sc}$ and the series resistance, R_s , defined by the slope of the J-V curve at $J = 0$.

About the effect of the thickness of the TBrTP films, Table 1 shows that the series resistance R_s decreases with the thickness, while the shunt resistance does not varies strongly. The strong R_s variation with the TBrTP thickness is due to its high resistivity. This large decrease of R_s justifies the increase of the performances of the OPVCs when the TBrTP thickness decreases. However, this positive effect is masked by the fact that the decrease of thickness implies a decrease of the absorption and thus of J_{sc} .

As shown in Table 1, replacing MoO₃ by MoO₃/CuI leads to a decrease of R_{sh} , while CuI increases significantly the conductivity of the TBrTP layer (Fig. 3), which results in a clear increase of J_{sc} .

When the thickness of the CuI layer is increased there is a strong degradation of V_{oc} and FF. In fact, if the presence of CuI allows improving J_{sc} , the shunt resistance of the OPVCs decreases when the CuI thickness increases.

Therefore, the high R_{sh} achieved with MoO₃ and better conductivity obtained with CuI explains the highest efficiency of the double anode buffer layer (DABL) MoO₃/CuI.

About the different morphologies of the organic film, it should be noted that the surface energy of the anode covered with MoO₃ is strongly higher than that of the anode covered with CuI [15, 16], which explains that the growth of the organic film is different. Moreover it is known that CuI exhibits a high reactivity with the sulphur, nitrogen of the organic molecules [18–22].

CONCLUSION

It is shown that simple porphyrin derivative, the TBrTP allows achieving OPVCs exhibiting promising efficiencies when the ABL is the MoO₃/CuI DABL. The CuI improves the current in the organic layer by one order of magnitude, which allows decreasing the series resistance of the OPVCs and therefore improving the OPVCs performances. On the other hand, MoO₃ allows

1 achieving high shunt resistance. All this makes that the
2 use of the DABL allows accumulating the positive effects
3 of each of ABL.

4 **Acknowledgements**

5 The authors thank project Fondecyt 3100066 and
6 project ECOS-CONICYT no. C09E02.
7
8
9

10 **REFERENCES**

- 11 1. <http://www.heliatek.com/>
- 12 2. Zeng W, Yong KS, Kam ZM, Zhu F and Li Y. *Appl.*
13 *Phys. Lett.* 2010; **97**: 133304.
- 14 3. Berredjem Y, Karst N, Cattin L, Lkhdar-Toumi A,
15 Godoy A, Soto G, Diaz F, del Valle MA, Morsli
16 M, Drici A, Boulmok A, Gheid AH, Khelil A and
17 Bernède JC. *Dyes Pigm.* 2008; **78**: 148–156.
- 18 4. Vilmercati P, Castellarin Cudia C, Larciprete R,
19 Cepek C, Zampieri G, Sangaletti L, Pagliara S,
20 Verdini A, Cossaro A, Floreano L, Morgante A,
21 Petaccia L, Lizzit S, Battochio C, Polzonetti G and
22 Goldoni A. *Surface Science* 2006; **600**: 4018–4023.
- 23 5. Cho EH, Chae SH, Kim K, Lee SJ and Joo J. *Syn-*
24 *thetic Metals* 2012; **162**: 813–819.
- 25 6. Peumans P, Bulovic V and Forrest SR. *Appl. Phys.*
26 *Lett.* 2000; **76**: 2650.
- 27 7. Song QL, Li FY, Yang H, Wu HR, Wang XZ, Zhou
28 W, Zhao JM, Ding XM, Huang CH and Hou XY.
29 *Chem. Phys. Lett.* 2005; **42**: 416.
- 30 8. Lare Y, Kouskoussa B, Benchouk K, Ouro Djobo S,
31 Cattin L, Diaz FR, Gacitua M, Abachi T, del Valle
32 MA, Amijo F, East GA and Bernède JC. *J. Phys.*
33 *Chem. Solids* 2011; **72**: 97–103.
- 34 9. Norrman K, Masen MV, Gevorgyan SA and Krebs
35 FC. *J. Am. Chem. Soc.* 2010; **132**: 16883–16892.
- 36 10. Bernède JC, Berredjem Y, Cattin L and Morsli M.
37 *Appl. Phys. Lett.* 2008; **92**: 083304.
- 38 11. Bernède JC, Cattin L, Ouro Djobo S, Morsli M,
39 Kanth SRB, Patil S, Leriche P, Roncali J, Godoy A,
40 Diaz FR and Del Valle MA. *Phys. Status Solidi A*
41 2011; **208**: 1989.
- 42 12. Zhou N, Guo X, Ortiz RP, Li S, Zhang S, Chang
43 RPH, Facchetti A and Marks TJ. *Sci. Adv. Mater.*
44 2012; **24**: 2242–2248.
- 45 13. Sullivan P, Jones TS, Ferguson AJ and Heutz S.
46 *Appl. Phys. Lett.* 2007; **91**: 233114.
- 47 14. Cheng CH, Wang J, Du GT, Shi SH, Du ZJ, Fan ZQ,
48 Bian JM and Wang MS. *Appl. Phys. Lett.* 2010; **97**:
49 083305.
- 50 15. Makha M, Cattin L, Ouro D, Sanoussi SN, Langlois
51 N, Angleraud B, Morsli M, Addou M and Bernède
52 JC. *Eur. Phys. J. Appl. Phys.* 2012; **60**: 31302.
- 53 16. Velez JH, Aguirre MJ, Zamora PP, Cattin L, Makha
54 M and Bernede JC. *Open J. Appl. Sci.* 2013; **3**:
55 136–144.
- 56 17. Lare Y, Godoy A, Cattin L, Jondo K, Abachi T, Diaz
57 FR, Morsli M, Napo K, del valle MA and Bernede
JC. *Appl. Surf. Sci.* 2009; **255**: 6615–6619.
- 18 Blake AJ, Brooks NR, Champness NR, Cooke PA,
19 Crew M, Deveson AM, Hanton LR, Hubberstey FP
20 and Schröder DM. *Cryst. Eng.* 1999; **2**: 181.
- 21 Lobana TS, Khanna S, Castineiras A, Hundal G and
22 Anorg Z. *Allg. Chem.* 2010; **636**: 454.
- 23 Gallego A, Castillo O, Gomez-García CJ, Zamora F
24 and Delgado S. *Inorg. Chem.* 2012; **51**: 718.
- 25 Song L-S, Wang Q-L and Niu Y-Y. *Synth. React.*
26 *Inorg., Met.-Org., Nano-Met. Chem.* 2011; **41**: 1080.
- 27 Fang Z-L, He J-G, Zhang Q-S, Zhang Q-K, Wu
28 X-Y, Yu R-M and Lu C-Z. *Inorg. Chem.* 2011; **50**:
29 11403.